Petrology of Shocked Clasts in an Anorthositic Lunar Breccia

Christian Anderkin [1, 2]

[1] *University of Florida Department of Geological Sciences, Gainesville, Florida*

[2] *Santa Fe College Department of Earth Sciences, Gainesville, Florida*

Email: atussex@gmail.com

Abstract: The analysis of mineral distribution within lunar breccia samples is invaluable in obtaining an immersive understanding of lunar crustal composition, as well as providing insight as to the diversity of geological activity apparent on the lunar surface. This petrologic study of 5 clasts within NWA 6355, an anorthositic lunar breccia, was conducted to assess the extent to which igneous granules displayed evidence of shock metamorphism before subsequent lithification. For this reason, a sample with a low composite shock grade was chosen [1]. Conclusions drawn from the characterization of clasts were extrapolated to provide conjecture about the mobility of lunar material due to impactor events. Both petrologic and geochemical methods were employed to assess compositional and shock characteristics, including optical mineralogy, scanning electron microscopy (SEM) back-scattered electron (BSE) imaging, and EDAX energy-dispersive x-ray spectrometry (EDS). The sample in question is an anorthositic polymict breccia (BULK At%: 42.14% O, 25.05% Si, 6.09% Al, 5.87% Ca, 6.46% Fe, 9.02% Mg) with numerous clasts of varying igneous compositions. Here, it was concluded that 2 of the 5 clasts observed exhibited shock characteristics that were likely to have been present before their compaction within the brecciated sample. This technique can be extrapolated to other, larger datasets to provide insight as to how lunar crustal material is affected by impactor events.

Key words: Lunar breccia; Shock metamorphism

1. Introduction: Given their origin as fragments of the moon's crust, lunar meteorites are particularly useful in the placement of mineralogical constraints on the moon's crustal composition. While crustal samples collected by the Luna and Apollo scientists also prove themselves valuable in this regard, the nature of brecciated lunar meteorites (i.e. a sufficiently energetic random impact event must occur for a specimen to become dislodged from the surface and ejected into space) has the ability to provide a potentially broader portrait of the moon's crustal-mineralogical composition.

Classified as a feldspathic breccia, the lunar meteorite NWA 6355 consists of a dark-grey vesicular interior with small white clasts littered throughout its devitrified matrix [1]. Minor mineral debris is dispersed heterogeneously throughout the specimen and consists of fine to medium-grained igneous minerals (predominantly olivine, magnesium-rich ilmenite, pyroxenes, and feldspathic minerals) accompanied by larger clasts of low-calcium pyroxene ($Fs_{37.5\text{-}61.2}$), pigeonite, augite, olivine ($Fa_{29.5\text{-}33.9}$), and plagioclase ($An_{91.6\text{-}96.1}$) [1]. The specimen itself is a polymict breccia composed of matrix and clastic minerals that originate from both the lunar highland terrain, as well as the lowland (basin) terrain—the former being characterized as predominantly felsic in composition and the latter being characterized as predominantly mafic in composition. This polymict texture is interpreted as the result of crustal fragmentation and lithification due to impactor events. In addition, the specimen is paired with NWA 4936, NWA 5406, and NWA 6221, given their near-identical texture, mineralogical composition, and bulk atomic percentages [1].

The current consensus as to the petrogenesis of lunar mineralogies (and ultimately, the lunar crust itself) is the model of a global magmatic ocean. This model carries the implication that much of the moon was once covered in a global ocean of magma that provided a mode for the homogenization of lunar silicate material [2]. Measurements of the amount of FeO/MnO-based mineralogical deviation from observed terrestrial normative values have shown that lunar meteorites display consistent ratios of FeO/MnO within minerals of similar composition [2]. Here, the compositional concentrations and effects of shock in individual igneous clasts will be assessed to determine the mobility of lunar silicate material (i.e. clasts that exhibit high ex-situ shock characteristics are assumed to have been ejected via an impactor from terrain characterized by different bulk compositions). Effects of shock will be determined as the result of either impactor events that occurred before the meteorite lithified (ex-situ), or compaction events that occurred after the dispersement of lunar material from its zone of origin (in-situ). It is interpreted that mineral clasts came from regions that were previously relatively homogenous, made heterogenous by the dispersement of silicate material by impactor events [2].

2. Samples and Methods: Igneous clasts from NWA 6355—a single lunar feldspathic breccia—were examined for characteristics of shock. The textural properties of said clasts were characterized by ZEISS scanning electron microscope (SEM) back-scattered electron (BSE) imaging. Mean weight and atomic percentages, as well as compositional components and chemical mappings of pyroxene and anorthositic feldspar were characterized through use of the EDAX energy-dispersive x-ray spectrometer (EDS). This characterization took place at the University of Florida's Department of Geological Sciences. Known compositions of unequilibrated lunar lithologies (both mafic and felsic) were employed as comparisons to brecciated material, given that no unbrecciated specimens were available for comparative analysis. The majority of clasts observed exhibited features consistent with shock and thermal metamorphism. These effects are indicative of the impact-induced metamorphism of clastic fragments dislodged from the lunar crust. To ascertain the lunar provenance of the clasts (rather than an asteroidal or terrestrial origin), a Welch's t-test between the observed and expected ratios of FeO/MnO was conducted using R statistical software. The results of this calculation are displayed in Table 1. Given the two-tailed P-value of 0.5677, it is inferred that there does not exist a statistically significant difference between the observed population and the expected population. Hence, it is necessary to proceed with the

FeO/MnO Ratios - Low-Ca Pyroxene

Group:	FeO/MnO Ratio (Observed)	FeO/MnO Ratio (Standard) [1]
Mean:	73.071	74.700
SD:	2.719	6.810
SEM	1.028	2.574
N	3	7
Two-tailed P-value	0.5677	No statistically significant difference between populations

{**Table 1:** Pyroxene-based FeO/MnO ratios exhibit no statistically significant difference between observed and expected results.}

assumption that the specimen is of lunar origin.

3. Matrix Petrology and Atomic Chemistry: NWA 6455 is a lunar breccia with a dark-grey matrix containing abundant light-grey subhedral and anhedral clasts of varying size—from microclasts and spherules of approximately 40 μm in diameter to larger single-crystal clasts of approximately 500 μm in diameter. The matrix is composed of a mafic, chemically heterogenous devitrified glass, where the presence of numerous microcrystalline grains is evident. In addition, the matrix exhibits a mildly vesicular texture, indicating points in the rock that were once occupied by a gas phase. This composition was detected via an energy-dispersive x-ray spectrometry (EDS) spot-based analysis. The spot-based EDS spectrum is provided for reference (Fig. 1). This and more are illustrated in Fig. 1 & 2.

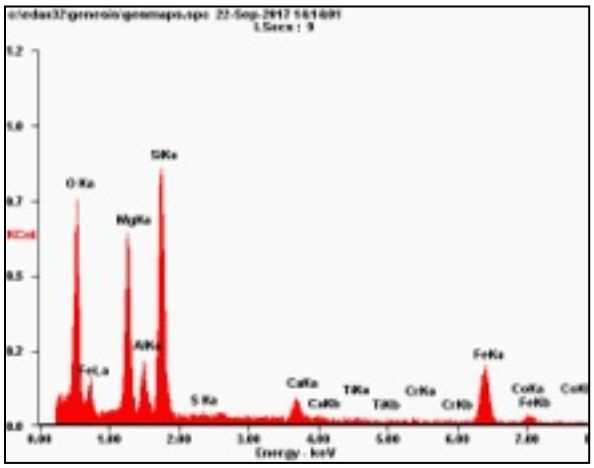

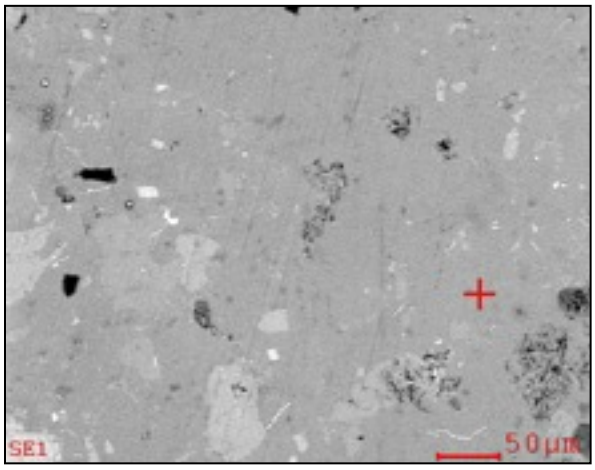

{**Fig. 1 & 2: 1.** This resulting spectrum from a matrix-based spot analysis yields a ferromagnesian composition. **2.** An image of the described sample plane captured via scanning electron microscope (SEM) back-scattered electron (BSE) imaging.}

The resultant spectrum from an individual EDS compositional spot analysis indicates that the matrix is of a mafic composition with average atomic weight percentages (At%) of 21.38% silicon, 39.95% oxygen, 16.71% magnesium, 4.07% aluminum, 2.08% calcium, and 14.50% iron. Elements with greater At% are indicated by spectral peaks. Here, matrix heterogeneity is introduced by the presence of abundant microcrystalline structures of varying chemical compositions. These are evident as structural and textural variances within the glassy matrix. Also noted is the matrix's minor vesicular texture. The matrix's composition closely resembles that of an Mg-rich inosilicate pyroxene, with substitutions of aluminum for silicon within the mineral's chain structure. This composition is contrasted by the spot analysis data provided in Fig. 3 & 4, which exhibits a less-ferromagnesian composition rich in aluminum and calcium.

For the second matrix-based spot analysis, the detected At% values for the aforementioned elements are 22.78% silicon, 45.26% oxygen, 4.67% magnesium, 15.72% aluminum, 2.08% calcium, and 1.07% iron. The existence of matrix-based heterogeneity underscores the sample's introduction of variance in matrix-based mineral compositions through the compaction of heterogenous lunar sediments. While this relative lack of homogenization superficially appears to contrast the notion of a global lunar magma ocean, it is far more likely representative of regular elemental zoning within minerals of dissimilar origin [2]. It is also important to note that the variations in matrix-based minerals are negligible in contrast to the variations between the matrix and clasts, as well as interclastal mineralogical differences.

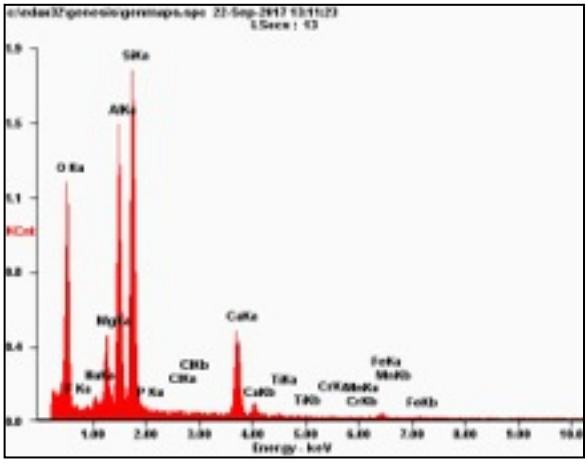

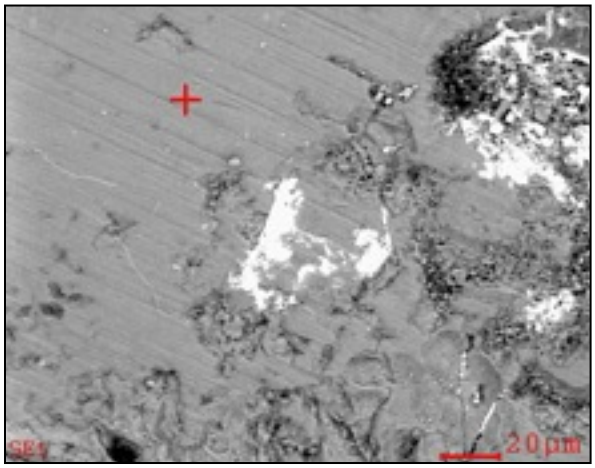

{**Fig. 3 & 4: 3.** The resulting spectrum from a second matrix-based spot analysis yields a less-ferromagnesian composition. Heterogeneity is here indicative of Mg/Fe zoning common in unequilibrated material. **4.** An image of the described sample plane captured via scanning electron microscope (SEM) back-scattered electron (BSE) imaging. Bright white Ilmenite ($FeTiO_3$) can be observed in the top-right corner of the image.}

4. Clastic Petrology and Chemical Composition:

Observed clasts exhibited a variety of coarsenesses, ranging from approximately 40 - 400 µm in diameter. Texturally, the clasts were of varying crystal size, and nearly all the observed clasts exhibited granoblastic amoeboid and typomorphic textures indicative of extensive shock metamorphism and deformation. In some unequilibrated pyroxene-rich clasts, this was evident as augite exsolution lamellae, but largely appeared in the form of dark shock veins.

4-1. Clast 1:

Clast 1 is a relatively large anhedral grain (~250 µm major-axis, 120 µm minor-axis) of calcium and magnesium-rich pigeonite pyroxene. Evident across the grain (parallel to the minor axis) are augite exsolution lamellae, evident of both fast cooling times and the augite-pigeonite miscibility gap. The detected At% for component elements are 24.89% silicon, 44.24% oxygen, 7.77% magnesium, 5.16% aluminum, 8.81% calcium, and 4.65% iron. It is inferred that while crystallization of the grain occurred, augite and pigeonite simultaneously precipitated from the parent melt and cooled at varying rates [3]. Since magnesium/calcium-rich pyroxenes are subject to higher liquidus temperatures than iron/calcium-rich pyroxenes (1200 C vs. 1050 C), crystal nucleation in Mg-rich compositions began before nucleation in Fe-rich compositions, resulting in the Fe/Mg zonation of high-Ca pyroxene [3]. Taking into account the relatively fast cooling time, it is inferred either that A.) the specified grain originated in an extrusive melt that experienced relatively fast cooling times and was subsequently subject to an impactor event that dislodged the grain as ejecta or B.) the grain was ejected as magma from an outcrop of equilibrated pyroxene that was melted upon impact and subsequently experienced Fe/Mg zonation. Given the anhedral shape of the grain, presence of shock veins along the grain's minor axis (shock veins would not be preserved if the grain were melted upon impact and then transferred and recrystallized), and lack of evidence of in-situ crystallization phases (illustrated in Fig. 6), the former is assumed.

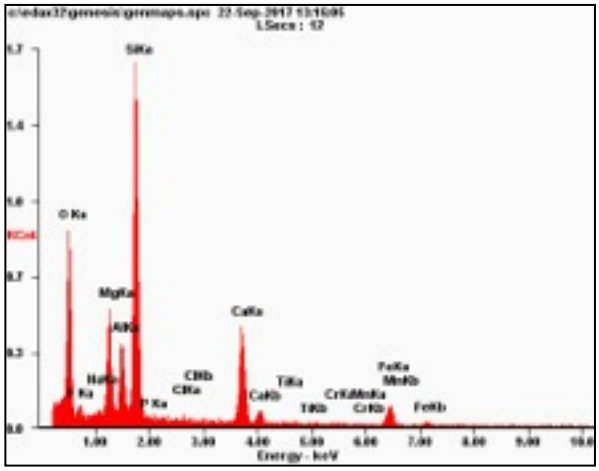

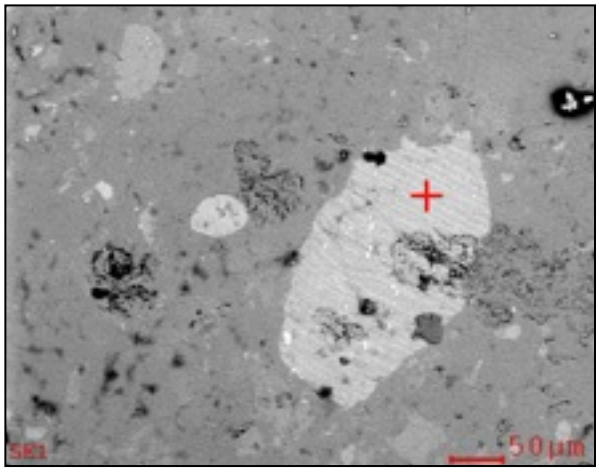

{**Fig. 5 & 6: 5.** The resulting spectrum from a single clastic spot analysis yields a Ca and Mg-rich composition. **6.** An image of the described sample plane captured via scanning electron microscope (SEM) back-scattered electron (BSE) imaging. Heterogeneity is here indicative of Mg/Fe zoning common in unequilibrated material. In addition, augite exsolution lamellae are visible as striations along the

minor-axis of the grain. Indicated here is a zone toward the core of the grain that is Mg-rich and depleted in Fe.}

4-2. Clast 2:

Clast 2 is a large anhedral anorthitic plagioclase grain with a major axis of approximately 500 µm and minor axis of approximately 300 µm. The most salient feature attributable to impact-assisted deformation is the set of large shock veins innervating the lower-left portion of the grain. Given the feldspathic nature of the clast, it is highly unlikely to have been derived from a similar parent melt as matrix-based components. It is further inferred that the observed grain was ejected from a highly felsic area of the moon, likely a portion of the lunar highland terrain [4]. The veins have been filled with a separate phase that appears darker in color, as well as glassier in texture. The detected At% for component elements of the anorthite grain are 18.35% silicon, 38.47% oxygen, 1.14% magnesium, 15.46% aluminum, 6.97% calcium, and 0.45% iron. The component elements here depict a feldspathic grain enriched with calcium and aluminum, and depleted in potassium, sodium, magnesium, and iron. The accompanying spectrum in Fig. 7 is representative of this.

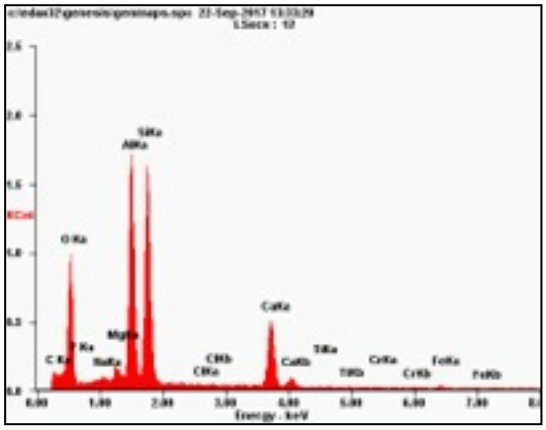

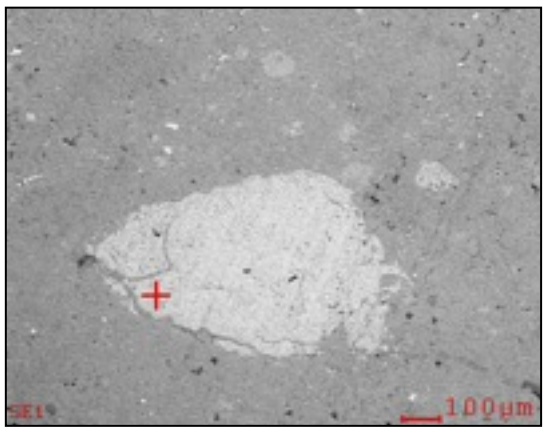

{**Fig. 7 & 8: 7.** The resulting spectrum from a single clastic spot analysis yields a Ca and Al-rich composition. **8.** An image of the described sample plane captured via scanning electron microscope (SEM) back-scattered electron (BSE) imaging. Shock veins occupied by an opaque phase are present in the lower-left corner of the grain.}

4-2.1. Phase Occupying Shock Vein

In addition to the spot analysis of the grain, a separate spot analysis was conducted on the vein itself to test the content of the phase occupying the shock vein's void space. The detected At% for component elements of the anorthite grain are 8.60% silicon, 39.20% oxygen, 4.92% magnesium, 4.34% aluminum, 15.14% calcium, and 3.15% iron. Given the peaks of oxygen, silicon, and calcium, it is presumed that the mineral innervating the grain of plagioclase is diopside ($CaMgSiO_3$). Due to the similarities between the phase in the shock vein and the matrix composition on a whole, it is concluded that the phase within the vein originates from a parent melt that is compositionally similar to the matrix. Taking into account their connectivity to the matrix itself, it is inferred that the metamorphic stress that created the shock veins occurred in-situ. These features are depicted in Fig. 9 and 10.

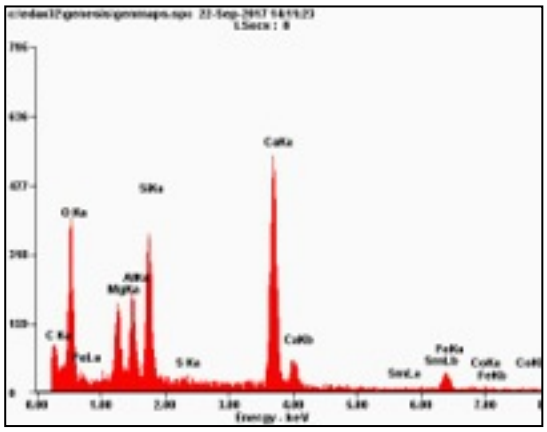

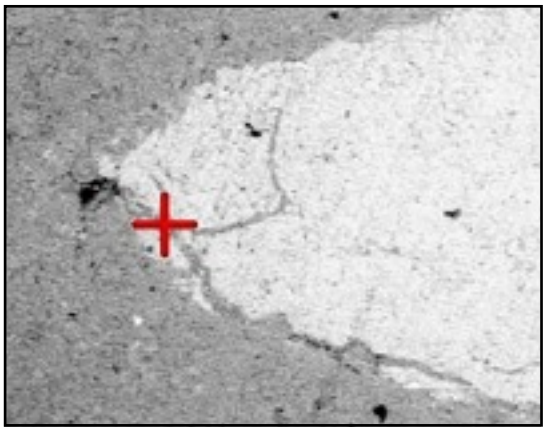

{**Fig. 9 & 10: 9.** The resulting spectrum from a single clastic spot analysis yields a vein of Wollastonite. **8.** An image of the described sample plane captured via scanning electron microscope (SEM) back-scattered electron (BSE) imaging. As in the case of Clast 1, the shock vein is preserved through transport of the grain. This, once again, carries the implication that the grain was not metamorphosed in situ. Note: the scale in Fig. 10 is preserved in Fig. 8.}

4.3. Clast 3:

Clast 3 is a medium-sized (~150 µm major axis, ~100 µm minor axis), highly metamorphosed grain of high-Ca pyroxene with shock veins present along its major axis. The void spaces within the veins are filled with ilmenite ($FeTiO_3$), which mobilized under immense pressure and heat. The detected At% for component elements of the pyroxene grain are 25.06% silicon, 44.19% oxygen, 9.02% magnesium, 5.09% aluminum, 4.87% calcium, and 6.46% iron. Given that high-Ca pyroxene has a much higher thermal ceiling than ilmenite (~1400 C for Ca-rich pyroxene and ~1050 C for ilmenite) [5,6], it can be extrapolated that the mineral experienced temperatures above 1050 C but not more than 1400 C. On the moon's surface, the most probabilistically likely source of intense heat and pressure within the described range (1050-1400 C) is an impactor event. The presence of reaction textures at the grain's boundaries leads to the assumption that the majority of the metamorphic stress the grain was subject to did not occur ex situ. The ilmenite in the upper-right corner of the clast exhibits mobility from an origin point in the matrix, to a point within the clast. This is indicative of high pressures and temperatures acting upon the ilmenite and forcing it into the shock veins of the clast.. This would not have been possible before the clast became contained within the matrix and is further indicative of in-situ shock metamorphism. The proposition that the clast is of a fragmental ejecta origin is strengthened by the presence of a separate high-Ca pyroxene microclast of identical texture and composition to the left of the main mass. The presence of two separate anhedral grains of varying size points to the position that the grains originated as ejecta from a common origin and were then subject to lithification.

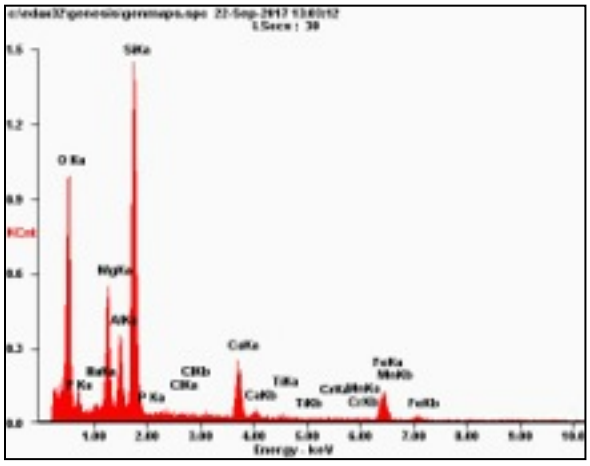

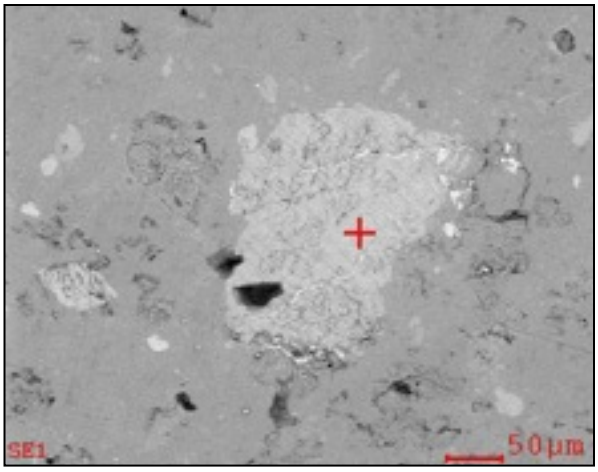

{**Fig. 10 & 11: 10.** The resulting spectrum from a single clastic spot analysis yields a vein of high-Ca pyroxene. **11.** An image of the described sample plane captured via scanning electron microscope (SEM) back-scattered electron (BSE) imaging. Note the mobility displayed by ilmenite. This oxide's mobility is indicative of temperatures near or above 1050 C. [6]}

4.4. Clast 4:

Clast 4 is a large anhedral low-Ca enstatite-pyroxene grain (~500 µm major axis, ~400 µm minor axis) that contains numerous shock veins. There exist no extra-clastal phases occupying the void spaces within evident fractures. The detected At% for component elements of the enstatite pyroxene grain are 26.21% silicon, 40.59% oxygen, 10.91% magnesium, 4.03% aluminum, 3.66% calcium, and 8.60% iron. Shock veins can be viewed running parallel to the grain's minor axis that terminate as they approach the clast-matrix boundary. This, combined with the lack of grain-matrix reaction textures and the largely anhedral shape of the clast suggests that the majority of metamorphic stress the grain was subject to was exerted upon it before or as it was ejected rather than by in-situ compaction events. This and more are illustrated in Fig. 12 & 13.

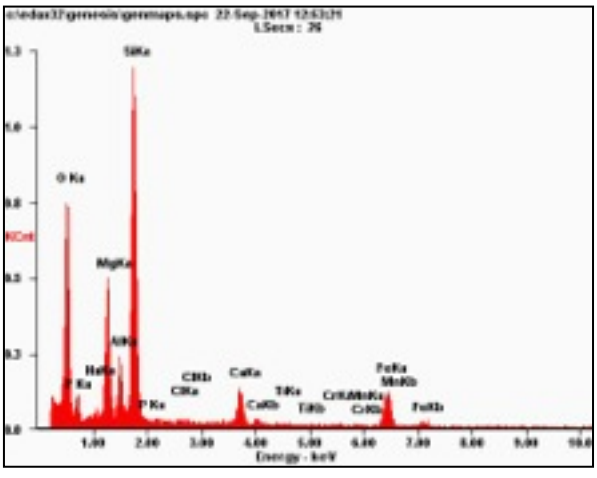

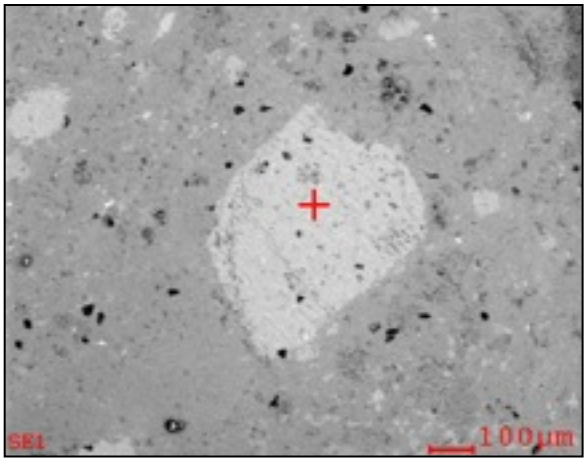

{**Fig. 12 & 13: 12.** The resulting spectrum from a single clastic spot analysis yields a vein of low-Ca enstatite pyroxene. **13.** An image of the described sample plane captured via scanning electron microscope (SEM) back-scattered electron (BSE) imaging.}

4.4. Clast 5:

Clast 5 is a small microclast of augite (~50 µm major axis, ~25 µm minor axis) with little evidence of ex-situ shock metamorphism. The detected At% for component elements of the pyroxene grain are 25.06% silicon, 42.94% oxygen, 12.82% magnesium, 5.78% aluminum, 2.99% calcium, and 5.28% iron. It exhibits a small fracture on the upper-left portion of the grain that begins just inside the granular boundary and extends outward into the matrix. This is indicative of in-situ fracturing, and does not provide information about the grain's metamorphic history previous to its lithification. Given that the breccia-focused mode of compaction is largely attributable to impactor events, it is possible that the fracture is of this origin. While it shares a similar composition to Clast 1 (mid-level Ca content/Mg-rich pyroxene), the lack of augite exsolution lamellae indicates that it did not likely precipitate from the same melt as Clast 1 [3]. This is illustrated in Fig. 15.

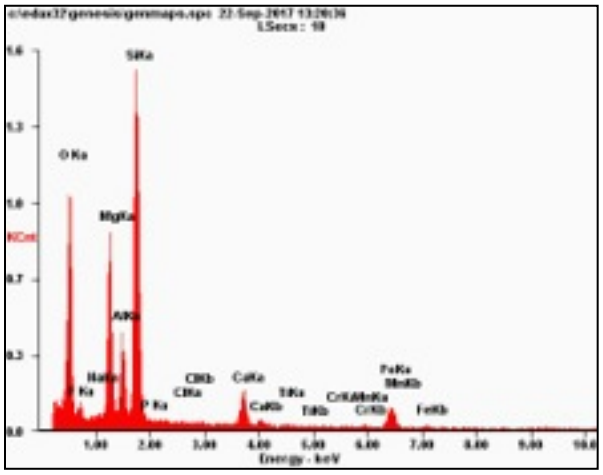

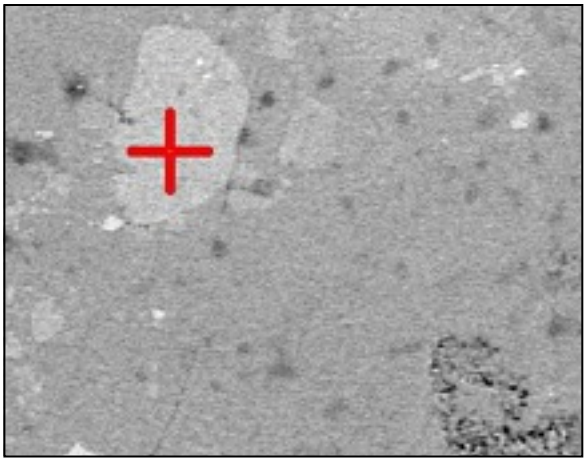

{**Fig. 14 & 15: 14.** The resulting spectrum from a single spot analysis yields a microclast of low-Ca augite pyroxene. **15.** An image of the described sample plane captured via scanning electron microscope (SEM) back-scattered electron (BSE) imaging. Note: The scale in Fig. 6 is preserved in Fig 15.}

5. Results:

Taking into account the lack of planetary heat engines within the moon, it is important to note that heterogeneity within NWA 6355 is due to the dispersion and subsequent compaction of lunar silicate material by impactor events, rather than by tectonics or volcanism. Through this process of impaction, mobility, and subsequent compaction, shock characteristics accumulate both within clastal domains as well as in the breccia itself. Here, evidence of shock metamorphism that is confined clasts is inferred to have occurred off-site (ex-situ), whereas shock characteristics that continuously occupy both the matrix and the clastal domains are inferred as having occurred after compaction (in-situ). Of the 5 grains assessed for ex-situ shock characteristics, clasts 1 and 4 exhibited characteristics that were consistent with the effects of off-site shock metamorphism and igneous activity. In addition, an EDS spot analysis of the core of Clast 1 yielded a chemically disparate composition to that of the matrix. Clast 4, while maintaining a compositional similarity to the matrix, exhibited isolated shock veins across its minor axis that terminated as they reached the matrix. This is indicative of off-site fracturing and by extent, mobility induced by an impactor.

6. Conclusions:

Given that the heterogeneity of lunar regolithic material is largely attributable to impact events on the moon's outermost crustal layers [4], it stands to reason that mobility induced by an impactor event can be assumed for the majority of breccia-based clasts. In the case of this petrologic research, it can be

reasonably ascertained that clasts 1 and 4 were subject to shock metamorphism before their compaction within the sample. While other clasts exhibited characteristics of shock metamorphism, the effects apparent in clasts 2, 3, and 5 are not discontinuous enough with the matrix to infer that shock metamorphism occurred in a locality separate from the sample. This is supplemented by the significant variances in elemental concentrations between the matrix and clasts, as well as between individual clasts.

7. References:

1. Meteoritical Bulletin: Entry for Northwest Africa 6355. (n.d.). Retrieved September 23, 2017, from https://www.lpi.usra.edu/meteor/metbull.php?code=52584

2. A. L. Turkevich, "The Average Chemical Composition of the Lunar Surface," Lunar Sci. Conf. 4, 1159–1168 (1973).

3. Yoder, H. (1952). Change of Melting Point of Diopside with Pressure. *The Journal of Geology, 60*(4), 364-374. Retrieved from http://www.jstor.org/stable/30058217

4. A. Bischoff, D. Weber, R. N. Clayton, et al., "Petrology, Chemistry, and Isotopic Compositions of the Lunar Highland Regolith Breccia Dar al Gani 262," Meteorit. Planet. Sci. 33, 1243–1257 (1998).

5. Barthelmy, D. (n.d.). Retrieved September 30, 2017, from http://webmineral.com/data/Enstatite.shtml#.Wc_JAxTzhSU

6. Barthelmy, D. (n.d.). Retrieved September 30, 2017, from http://webmineral.com/data/Ilmenite.shtml#.Wc_IuRTziFI